

A metric for characterization of two-dimensional spatial coherence

Daniel C. Brown, Cale F. Brownstead, and Thomas B. Gabrielson

*Applied Research Laboratory, The Pennsylvania State University, P.O. Box 30,
State College, Pennsylvania 16804, USA
dan.brown@psu.edu, cfb102@psu.edu, tb3@psu.edu*

Anthony P. Lyons

*Center for Coastal and Ocean Mapping, University of New Hampshire, Durham,
New Hampshire 03824, USA
anthony.lyons@ccom.unh.edu*

Abstract: A metric is developed providing a quantitative measure of the two-dimensional spatial coherence of scattered fields. The metric is based on fitting a function similar to bivariate Gaussian to measured two-dimensional coherence surfaces. This function provides a robust fit to the measured data for a range of coherence lengths and surface asymmetries. Through an eigendecomposition of the bivariate Gaussian covariance matrix, it is possible to define surface orientation as well as coherence lengths along the major and minor axes. The metric is applied to normal-incidence scattering data collected in recent field trials at Seneca Lake, NY.

© 2017 Acoustical Society of America
[LMZ]

Date Received: May 30, 2017 **Date Accepted:** August 22, 2017

1. Introduction

Most measurements of the spatial coherence of acoustic fields are made using a one-dimensional linear array.¹ The spatial coherence is measured by calculating a metric, such as correlation coefficient, through pairwise comparisons of the elements within the array. This produces a one-dimensional measure of the correlation coefficient versus the spatial hydrophone separation. The measured spatial coherence typically falls from a peak at zero offset. A first-order approximation to the spatial loss of coherence is the “coherence length,” which is commonly defined as the distance required for the coherence to fall to $1/e$ of the peak value.

There are a number of domains where the spatial coherence of the field scattered from the seafloor plays an important role. These areas include synthetic aperture sonar image formation, acoustic seafloor characterization, and array gain modeling. To characterize the spatial coherence, many measurements have been made of horizontal and vertical coherence of underwater acoustic fields.^{2–4} Simultaneous measurement of the two-dimensional spatial coherence is less common, and characterization of the coherence length in the “off-axis” (i.e., non-horizontal or non-vertical) directions is even less common. Correlation Velocity Log (CVL) sonar systems are an exception. These systems utilize a two-dimensional receive array to measure the two-dimensional spatial coherence of the acoustic field scattered near normal incidence. CVL velocity estimation requires accurate measurement of the two-dimensional spatial coherence of the scattered field. It can be shown that the CVL’s accuracy is proportional to the coherence length of the received field.^{5,6} The measured two-dimensional spatial coherence is not guaranteed to have radial symmetry; therefore, the standard univariate coherence length measure is inadequate for CVL error modeling.

In this work, a metric for the two-dimensional spatial coherence is developed and applied to field data collected at Seneca Lake, NY. A brief description of the test area, the sonar system, and the associated signal processing are provided in the following section. A metric for the two-dimensional spatial coherence is given in Section 3. This metric provides a pair of measures of the coherence length and a separate measure of the surface orientation. The metric is applied to field data and it is shown to provide adequate flexibility to describe the shape of the surface while requiring the estimation of only four free parameters.

2. Experimental measurements of spatial coherence

The acoustic testing described here was conducted on June 18, 2015 at Seneca Lake, NY. Seneca Lake is 1 of 11 lakes located in an area of New York State known as the

Finger Lakes region. It is the largest by volume of these lakes with a 186 m maximum depth, a 57 km length and a 5 km width at its widest point.⁷ Testing was conducted in a central portion of the lake where the water depth is roughly 180 m. The sonar data collected along a test track is processed to produce a sub-bottom profile showing the lake bathymetry and sub-bottom sediment structure, Fig. 1. This track runs north-to-south and the lake floor and the sub-bottom layers are sloped less than 0.5° . Additional testing in this area of the lake has shown that the east-to-west slope of the lake floor is less than 1.0° .

The sonar system used to collect this data consists of a 48 element receive array and a single channel projector mounted to a sonar frame attached to a 9 m pontoon boat. The receive array consists of 48 hydrophones arranged in a rectangular 6-element by 8-element grid with a 9.14 cm center-to-center spacing. The sonar system transmits a linearly frequency modulated waveform from 12 to 24 kHz with a pulse length of 10 ms. This waveform is windowed with a 10% Tukey window.⁸

For each transmitted pulse, a 100 ms record is segmented from the signals recorded on the hydrophone array. This 100 ms record begins at the onset of the first return from the lake bed. A 16–20 kHz bandpass filter is applied to these signals. After segmentation and filtering, a temporal window is applied so the spatial coherence can be evaluated for different portions of the return signal. The coherence is then measured by calculating the zero-lag correlation coefficient for each of the possible 48^2 element pairs.

Each of these correlation measures has an associated spatial offset; however, these offsets are not unique. For example, the 48 autocorrelations all represent zero spatial offset. Examination of the array layout and the redundant spatial offsets shows that for a fully populated rectangular array with dimensions m by n there are $(mn)^2$ correlation pairs with $(2m - 1)(2n - 1)$ unique spatial offsets. Therefore, the 6×8 element receive array used in this experiment produces an 11×15 array of unique spatial offsets. Mapping from a large number of element pairs (48^2) to the smaller number of unique spatial offsets (11×15) has been discussed in the context of correlation velocity log signal processing by Boltryk *et al.*⁹

This mapping is applied to the data collected at Seneca Lake and the results are shown in Fig. 2. This figure includes an isolevel overlay along with a number of metrics in its title. These will be discussed in Sec. 3. Here, it is worth noting that this spatial representation of the data permits an intuitive interpretation of the measured correlation coefficients. The two-dimensional spatial coherence surface has a peak at zero displacement. The surface is asymmetric and the correlation coefficient falls monotonically in the region near the peak.

3. A metric for the two-dimensional spatial coherence

A coherence length measure is needed for the spatial coherence surface shown in Fig. 2. The presence of surface asymmetry requires a new metric to describe the asymmetric

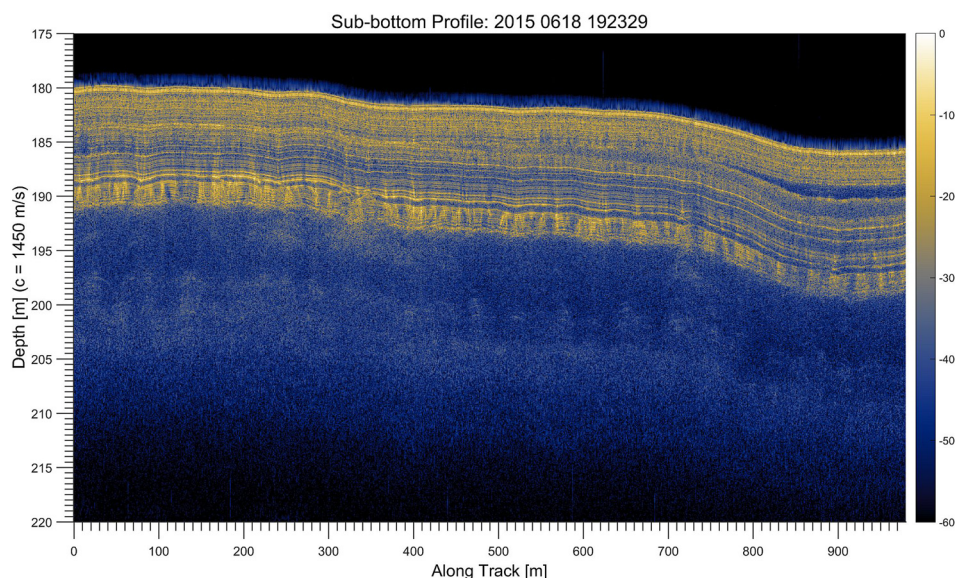


FIG. 1. (Color online) This sub-bottom profile of the lake bed is collected on a North-to-South track near the center of Seneca Lake, NY. This profile is generated from 1000 sequential pings where the sonar system advances approximately 1 m per ping. The data is shown on a 60 dB color scale indexed to the peak value.

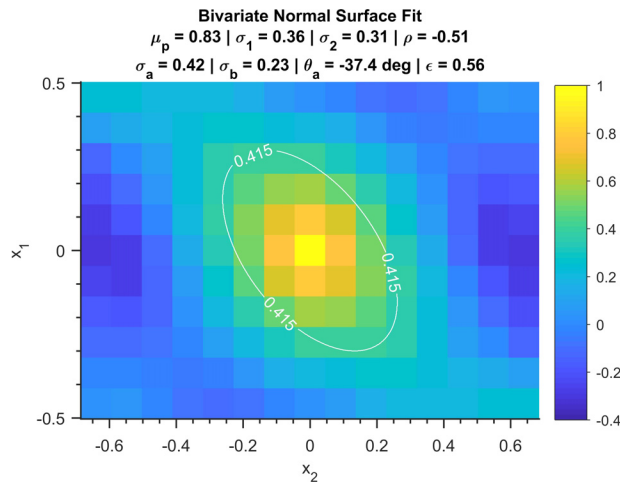


FIG. 2. (Color online) The correlation coefficients measured by a two-dimensional receive array are shown, where the spatial dimensions are in meters. The bivariate normal surface fit is applied to the data and the fit parameters are shown in the title. A thin white isoline is shown at the level equal to half the estimated peak value.

coherence length and surface orientation. The remainder of this paper will focus on the development of a metric for the spatial coherence measured by a two-dimensional array and a single transmitted pulse.

The shape of the surface is characterized by fitting a function with a form similar to a two-dimensional Gaussian to the measured coherence surface. This fitting process will be called the “bivariate normal surface fit.” This function provides a reasonably flexible two-dimensional shape for fitting those cases where the measured coherence falls monotonically from the peak value. The fit is less accurate when the coherence does not fall monotonically; however, it still provides a useful measure of the width and asymmetry present near the peak of the spatial coherence. The functional form used to fit to the measured data is given by

$$\mu = \mu_p \exp \left\{ -\frac{1}{(1 - \rho^2)} \left[\left(\frac{x_1}{\sigma_1} \right)^2 + \left(\frac{x_2}{\sigma_2} \right)^2 - 2\rho \frac{x_1 x_2}{\sigma_1 \sigma_2} \right] \right\}, \quad (1)$$

where σ_1 and σ_2 are the widths of the spatial coherence along the respective axes, ρ provides a measure of asymmetry and surface orientation, and μ_p is the peak of the bivariate function that is fit to the measured correlation coefficients. This function is fit to the measured spatial coherence surface using nonlinear least squares regression (specifically MATLAB `nlinfit.m`),¹⁰ where σ_1 , σ_2 , ρ , and μ_p are the estimated coefficients. Note that, in implementation, the auto-correlation channel pairs should be excluded from the fit process. These channels will always show perfect correlation; therefore, they provide no additional information. In the case of a data collection with low signal to noise ratio, the ambient noise will bias the cross-correlation coefficients to zero while the auto-correlation coefficient will remain one. If the auto-correlation channels are not excluded from the fit process in low SNR cases, the resulting correlation lengths estimates will be biased.

One weakness of this approach is in the intuitive understanding of the degree of surface asymmetry. If the surface is perfectly symmetric, then $\sigma_1 = \sigma_2$ and $\rho = 0$. However, if the surface is asymmetric the degree of asymmetry and orientation are both encoded in σ_1 , σ_2 , and ρ . Combining multiple separate measures to describe the asymmetry is confusing and leads to a more difficult interpretation of the results. To resolve this issue, a second set of coherence lengths are calculated, and these new lengths are oriented along the major and minor axes of the asymmetric surface.

To calculate these surface aligned coherence lengths, begin by expressing Eq. (1) in vector notation as

$$\mu = \mu_p \exp \{ -\mathbf{x}^T \Sigma^{-1} \mathbf{x} \}, \quad (2)$$

where $\mathbf{x} = [x_1 \ x_2]^T$, where x_1 is the forward direction and x_2 is the athwartship direction. The covariance is

$$\Sigma = \begin{bmatrix} \sigma_1^2 & \rho\sigma_1\sigma_2 \\ \rho\sigma_1\sigma_2 & \sigma_2^2 \end{bmatrix}. \quad (3)$$

The eigendecomposition of the covariance matrix is $\Sigma = U\Lambda U^\top$, where the columns of U are the eigenvectors of Σ and Λ is a diagonal matrix whose entries are the corresponding eigenvalues. Defining $\mathbf{z} = U^\top \mathbf{x}$, the coherence length is found by setting the argument of the exponential in Eq. (2) equal to -1 . This gives

$$\mathbf{z}^\top \Lambda^{-1} \mathbf{z} = 1. \quad (4)$$

This equation can be rewritten in a simple algebraic form as

$$\frac{z_a^2}{\lambda_a} + \frac{z_b^2}{\lambda_b} = 1. \quad (5)$$

The $1/e$ isolevel of a bivariate Gaussian is an ellipse with major and minor axes lengths of $\sigma_a = \sqrt{\lambda_a}$ and $\sigma_b = \sqrt{\lambda_b}$, respectively. To summarize, the matrix U forms an orthonormal basis that is oriented with its axes relative to the surface. The operation, $\mathbf{z} = U^\top \mathbf{x}$, projects the surface from the array aligned coordinate system (\mathbf{x}) to the surface aligned coordinate system (\mathbf{z}).

The surface-aligned coherence lengths are found through an eigendecomposition of the covariance matrix used to describe the bivariate normal surface. The resulting eigenvectors are oriented along the major and minor axes of the surface and the eigenvalues are equal to the square of the coherence lengths along these axes. The major axis coherence length is given by σ_a and the minor axis coherence length is given by σ_b . The orientation of these axis are denoted by the angle θ_a , where $\theta_a = 0$ indicates that the major axis is aligned with the x_1 axis. Therefore, if $\theta_a = 0$ then $\sigma_a = \sigma_1$ and $\sigma_b = \sigma_2$. Using the coherence lengths aligned to the major and minor axes it is possible to define a single measure of the surface asymmetry

$$\epsilon = \frac{\sigma_b}{\sigma_a}. \quad (6)$$

This measure of asymmetry is bounded such that $\epsilon \in (0, 1]$, because the major axis coherence length, σ_a , is always greater than the minor axis coherence length, σ_b . $\epsilon = 1$ is the case of no asymmetry (a circular surface) and the most extreme asymmetry occurs as $\epsilon \rightarrow 0$.

The bivariate normal fit has been applied to the data shown in Fig. 2, and the fit parameters shown within the title. A thin white isolevel line is shown at half the estimated surface peak value. This line is useful as a tool for visualizing the asymmetry and qualitatively judging the fit to the underlying function. In this case, the surface shows moderate asymmetry $\epsilon = 0.56$ with an orientation of $\theta = -37.4^\circ$. The surface fit function has well approximated the width and orientation of the central portion even with a non-monotonically decreasing surface at the largest spatial offsets.

This metric was applied to the data collected near 408 m along-track in the sub-bottom profile shown in Fig. 1. The data was segmented from the 100 ms record using 10 ms temporal windows with four window start times from 0 to 30 ms in 10 ms steps. The purpose of the experiment was to study the effect of the sediment structure on the coherence length. Using short temporal windows, it was possible to restrict analysis to specific regions of the sub-bottom. The spatial coherence can be associated with the distinct layering seen in the sub-bottom profile.

A spatial coherence surface for each of the four temporal windows applied to the selected ping is shown in Fig. 3. The shape of the surface was measured using the bivariate normal fit and the fit parameters are provided in the title of each figure. Generally, the surfaces narrow with increasing time and they are moderately asymmetric. The earliest two windows span the uppermost, layered sequence. The coherence lengths for these windows are relatively large and they show asymmetry oriented where $\theta_a > 0$. The orientation abruptly changes to $\theta_a < 0$ for the later pair of intervals. This change occurs as the temporal window passes beyond the uppermost sediment sequence and into the more isotropic sub-bottom below.

This metric has been calculated for each of the 1000 pings making up the sub-bottom profile shown in Fig. 1. The surface aligned coherence lengths, σ_a and σ_b , are shown in Fig. 4 for the 0–10 ms temporal window. The major axis coherence length varies from 0.7 to 2.0 m and the minor axis length varies from 0.3 to 1.5 m. The asymmetry varies with ϵ ranging over 0.3–1.0. Visual assessment of the fit quality found the metric accurately tracking the shape and orientation of the coherence surface throughout the dataset.

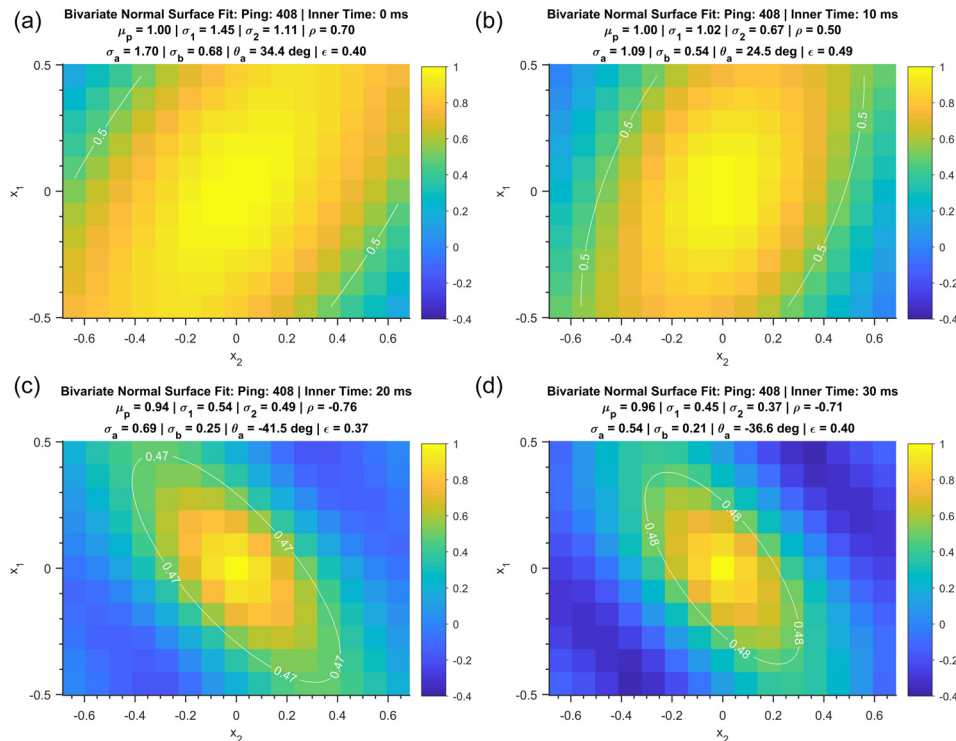


FIG. 3. (Color online) The spatial coherence surface is shown for ping 408 of track 192329 for a temporal window with a 10 ms length. Like Fig. 2, the spatial dimensions are shown in meters. The temporal windows for each figure begin at (a) 0 ms, (b) 10 ms, (c) 20 ms, and (d) 30 ms. The shape of each surface is measured using the bivariate normal fit and the fit parameters are provided in the title of each figure.

Note that the analysis presented in this paper has focused on the real component of the complex correlation coefficient. Caution should be exercised if this metric is applied to the magnitude of the complex correlation coefficient. The estimate of the magnitude of the complex correlation coefficient is highly biased for low signal coherence.¹¹ If this bias is not taken into account prior to application of this metric, the resulting coherence length estimates will be biased.

4. Conclusion

An experiment at Seneca Lake, NY measured the normal-incidence field scattered from the lake bed. This data was processed to calculate the two-dimensional spatial coherence, which was found to have significant variability between pings and between temporal windows. The use of a single coherence length measure was inadequate to characterize the width and orientation of the measured surfaces. A two-dimensional metric, based upon a surface fit, was developed to address this shortcoming.

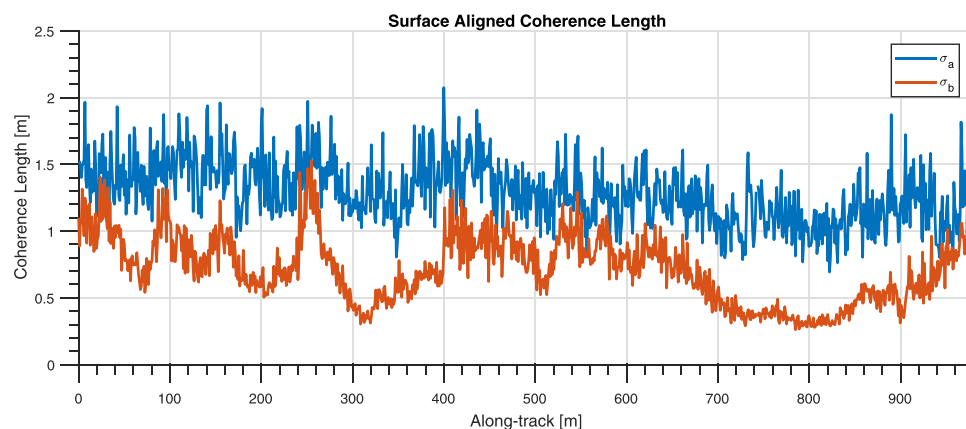


FIG. 4. (Color online) The surface aligned coherence lengths, σ_a and σ_b , are shown for the earliest 10 ms of lake bed returns in Fig. 1. The coherence length and asymmetry vary significantly over this track. Note that ping 408 analyzed in Fig. 3 is near 408 m along-track.

The proposed metric was applied to the experimental data. The recorded data was segmented into four sequential temporal windows, and the two-dimensional spatial coherence was calculated for each temporal interval. The spatial coherence varies significantly between temporal windows, and it appears sediment layering properties of the lake bed have a strong influence on the observed spatial coherence. Across all the cases shown, the proposed metric accurately captured the coherence length asymmetry and orientation.

The proposed measure of the spatial coherence has several advantages. First, the shape of the bivariate Gaussian approximates the asymmetry observed in the measured surfaces accurately. Second, this metric is useful for two-dimensional arrays with a relatively small number of hydrophones since the fit process requires the estimation of only four free parameters. Finally, through an eigendecomposition of the Gaussian covariance matrix it is possible to measure the surface orientation and the surface-aligned coherence lengths. These surface aligned lengths may then be used to quantitatively assess the asymmetry of the spatial coherence surface.

Acknowledgments

The authors would like to acknowledge the U.S. Office of Naval Research for their support of this research. This work was conducted under the following grants and contracts Nos. N00014-15-G-0001/0009, N00014-14-1-0566, and N00014-16-1-2313.

References and links

- ¹W. M. Carey, "The determination of signal coherence length based on signal coherence and gain measurements in deep and shallow water," *J. Acoust. Soc. Am.* **104**(2), 831–837 (1998).
- ²G. R. Wilson, "Comparison of the measured covariance of surface reverberation for horizontal and vertical arrays," *J. Acoust. Soc. Am.* **72**(6), 1905–1910 (1982).
- ³D. R. Jackson and K. Y. Moravan, "Horizontal spatial coherence of ocean reverberation," *J. Acoust. Soc. Am.* **75**(2), 428–436 (1984).
- ⁴P. H. Dahl, "Forward scattering from the sea surface and the van Cittert-Zernike theorem," *J. Acoust. Soc. Am.* **115**(2), 589–599 (2004).
- ⁵F. R. Dickey and J. A. Edward, "Velocity measurement using correlation sonar," in *Proceedings IEEE Position Location and Navigation Symposium*, San Diego, CA (November 1978), pp. 255–264.
- ⁶D. C. Brown, "Modeling and measurement of spatial coherence for normal incidence seafloor scattering," Ph.D. dissertation, The Pennsylvania State University, State College, PA, 2017.
- ⁷J. D. Halfman, "Water quality of Seneca Lake, New York: A 2011 update," Technical Report Hobart and William Smith Colleges, Geneva, NY, 2011, available at <http://people.hws.edu/halfman/Data/2011%20Seneca%20Report%20v2.pdf>.
- ⁸F. Harris, "On the use of windows for harmonic analysis with the discrete Fourier transform," *Proc. IEEE* **66**, 51–83 (1978).
- ⁹P. J. Boltryk, M. Hill, A. C. Keary, and P. R. White, "Surface fitting for improving the resolution of peak estimation on a sparsely sampled two-dimensional surface with high levels of variance, for an acoustic velocity log," *Meas. Sci. Technol.* **15**, 581–591 (2004).
- ¹⁰MATLAB, 9.0.0.341360 (R2016a) (The MathWorks Inc., Natick, MA, 2016).
- ¹¹G. C. Carter, C. H. Knapp, and A. H. Nuttall "Statistics of the estimate of the magnitude-coherence function," *IEEE Trans. Audio Electroacoust.* **21**(4), 388–389 (1973).